Analytical Methods

ROYAL SOCIETY OF CHEMISTRY

PAPER

View Article Online
View Journal | View Issue

Cite this: *Anal. Methods*, 2022, **14**, 1051

Broad-specificity time-resolved fluorescent immunochromatographic strip for simultaneous detection of various organophosphorus pesticides based on indirect probe strategy

Haowei Dong,[abc] Deyan Xu,[abc] Guanjie Wang,[abc] Xiaoya Meng,[abc] Xia Sun,[abc] Qingqing Yang,[abc] Yemin Guo *[abc] and Yelong Zhu[d]

The massive use of organophosphorus pesticides (OPs) poses a great threat to food safety, human health and environmental protection. As there are many kinds of pesticides, their detection is facing a severe challenge. The simultaneous detection of multiple organophosphorus pesticides in one test is a problem to be solved at present. In this paper, a time-resolved fluorescent immunochromatographic (TRFIA) strip is prepared by using broad-specificity antibodies (Abs) of OPs as the recognition element. Abs were connected to europium oxide latex microspheres using sheep anti-mouse antibodies (SaMIgG) to form an indirect probe. This strategy could effectively realize signal amplification, and could save the amount and protect the activity of Abs. After the detection, the color change of the test line (T-line) was observed to make qualitative judgment under UV-light (365 nm). Then, the images of the positive sample were analyzed by using ImageJ to complete the quantitative detection. Under optimal construction and operating conditions, the limit of detection of the strip could reach 0.53 ng g^{-1}. And the TRFIA strip performed well in the additive test of vegetable samples. It is inexpensive to prepare, convenient to carry, and easy to operate. More importantly, it improves the detection efficiency and meets the needs of rapid field testing of a large number of samples.

Received 14th January 2022
Accepted 7th February 2022

DOI: 10.1039/d2ay00067a

rsc.li/methods

1 Introduction

Organophosphorus pesticides (OPs) are the most common pesticides in agricultural production. They are widely used due to their high efficiency and broad spectrum.[1,2] The use of OPs plays a very important role in ensuring food supply and improving the quality of agricultural products. OPs have nerve toxicity, and after entering the body, they will be combined with acetylcholinesterase hydroxyl and lead to phosphorylation. After phosphorylation, the activity of acetylcholinesterase is inhibited and acetylcholine cannot be effectively decomposed.[3,4] Eventually, excessive accumulation of acetylcholine in the body leads to neurotoxicity, thus acting as an insecticide. Because of the variety of OPs and the differences in residual levels, the detection of OP residues is confronted with great challenges.[5,6] At the same time, some producers use OPs in an irregular way to increase the growth rate of crops, resulting in excessive and residual problems that pose a serious threat to food safety.[5] This not only affects the production quality and safety of agricultural products, public health and sustainable development of the environment, but also hinders the development of the agricultural product export trade industry to a certain extent.[2,5] In China, the permissible limit (GB 2763-2016) of organophosphorus pesticides in vegetables is 10–100 ng g^{-1}.

Traditional detection methods include gas chromatography, mass spectrometry, high performance liquid chromatography and their combined methods. They are sensitive, specific, accurate and reliable.[7] The application and popularization of these methods are hindered by the complexity of sample pretreatment, time-consuming testing process and the need for professional operation.[6,8] Some new detection technologies (such as immune sensors, enzyme sensors, aptamer sensors, *etc.*) have been widely considered by some researchers because of their portability, rapidity, accuracy and efficiency, and due to their good detection effect in practical application.[9–11] The detection method of organophosphorus pesticides based on enzyme inhibition is relatively mature, easy to operate, has short detection time and low detection cost. However,

[a]*School of Agricultural Engineering and Food Science, Shandong University of Technology, No. 266 Xincun Xilu, Zibo 255049, China. E-mail: gym@sdut.edu.cn; Fax: +86 533 2786558; Tel: +86 533 2786558*

[b]*Shandong Provincial Engineering Research Center of Vegetable Safety and Quality Traceability, No. 266 Xincun Xilu, Zibo 255049, China*

[c]*Zibo City Key Laboratory of Agricultural Product Safety Traceability, No. 266 Xincun Xilu, Zibo 255049, China*

[d]*Zhenjiang Sanlong Ecological Agriculture Development Company Limited, Rongbing Quyang Village, Zhenjiang 212001, China*

carbamate pesticides also have similar enzyme inhibition, which will interfere with the detection results to a certain extent.[10] In addition, the pretreatment conditions of enzyme inhibition sensing methods are mainly aqueous phase,[12] which makes the extraction efficiency of pesticide residues low and restricts the improvement of detection performance of this method. Aptamers are easy to synthesize, with good repeatability and low preparation cost.[13] As emerging sensitive recognition elements, aptamers are widely used in OP detection. However, the currently known aptamer sequences that can identify organophosphorus pesticides with broad spectrum are limited, which to some extent hinders the in-depth exploration and promotion of aptamer sensors.[10,13] Among them, the rapid detection method established with broad-specificity antibodies (Abs) as core recognition elements provides a new idea for the preliminary detection of a large number of samples.[14] Abs achieve broad-specificity recognition by recognizing the common structure of one or several kinds of substances, in which the common structure is an antigen or a hapten.[15] Xu *et al.*[15–17] designed and synthesized four kinds of antigens with different structures for *O*,*O*-diethoxy OPs, and obtained Abs against *O*,*O*-diethoxy OPs through hybridoma technology. Based on these studies, they established direct competitive enzyme-linked immunoassay (dcELISA), direct competitive chemiluminescence enzyme-linked immunoassay (dcCLEIA), fluorescence polarization immunoassay (FPIA), direct competition time-resolved fluorescence immunoassay (dcTRFIA) and other immunoassay methods. Since the corresponding epitope is a common structure of various OPs, the Abs have the ability of broad-specificity recognition. The rapid detection method using Abs is still in the exploratory stage.

In recent years, time-resolved fluorescence immunochromatographic (TRFIA) strip assay, as a field detection technology with simple operation and low cost, has attracted extensive attention from researchers.[1,18] The Eu element can effectively reduce the background interference of traditional labelling materials (such as fluorescent dyes, enzymes, and gold nanoparticles).[19–21] Europium oxide latex microspheres prepared with the Eu element can emit orange-red fluorescence under UV-light of 365 nm.[22] Most TRFIA strips often use europium oxide latex microsphere as marking materials,[23] and specific biological materials (such as antibodies and aptamers) as core recognition elements, which are coupled to form detection probes.[24,25] Under the action of chromatography, a specific binding immune reaction occurs with the corresponding target substance intercepted and fixed on a nitrocellulose (NC) membrane. As the number of probes is increased, the lines show different intensities of colors or fluorescence signals. Traditional TRFIA strips label the signal material directly on the target antibodies, which is the direct probe strategy. In the actual detection work, too much target antibody consumption will increase the preparation cost, while too little target antibody will reduce the sensitivity and even result in a 'false negative'. In the case of certain detection ability and limited number of target antibodies, the indirect probe strategy can effectively amplify the fluorescence signal and improve the detection sensitivity of the TRFIA strips.[26] In this method, the target antibodies are indirectly coupled with europium oxide latex microspheres through multiple secondary antibodies [such as sheep anti-mouse antibodies (SaMIgG), rabbit anti-sheep antibodies (RaSIgG), *etc.*], so that the fluorescence signal of unit antibodies in the entire detection system is much higher than that of the traditional method.[25–27] Majdinasab *et al.*[27] have successfully established a rapid detection technique for ochratoxin detection using the indirect probe strategy. The limit of detection (LOD) of the indirect probe strategy was 0.4 pg g^{-1}, which was 100 times higher than that of the direct probe strategy. It should be noted that the application of the indirect probe strategy to other chromogenic nanomaterials is also significant. Urusov *et al.*[21] proposed an indirect probe strategy using gold nanoparticles as markers. The results showed that the sensitivity of the indirect labeling method in mycotoxin analysis was 20 times higher than that of traditional methods. The reduction of detection limit ranges from 5 times to 3 orders of magnitude. On the one hand, the indirect probe strategy can reduce the consumption of target antibodies. On the other hand, the secondary antibodies take the place of the target antibodies to participate in the complicated coupling steps, which can protect the biological activity and recognition ability of the target antibodies.

In this study, with OPs as the target and Abs as the sensitive recognition element, a TRFIA strip based on the indirect probe strategy was constructed. First, SaMIgG was bonded to europium oxide latex microspheres to prepare time-resolved fluorescent probes (Eu-SaMIgGs). Then, Abs were indirectly connected to europium oxide latex microspheres by specific recognition with SaMIgG, that is, the indirect time-resolved fluorescent probe (Eu-SaMIgGs-Abs) was prepared. Then OPs-BSA and RaSIgG were immobilized on a NC membrane successively. Qualitative judgment was made by monitoring the color change of the test line (T-line), and quantitative detection was realized by analyzing the gray value of the T-line with ImageJ software. In addition, we also optimized the construction and working conditions of the TRFIA strip to explore the response relationship between the gray value of the T-line and the concentration of OPs. And the detection effect of the strip in different sample matrix solutions was explored.

2 Experimental

2.1 Reagent

OPs-BSA, Abs, SaMIgG and RaSIgG were obtained from Beijing Biodragon Immunotechnologies Co., Ltd. (Beijing, China). Bovine serum albumin (BSA) and 1-(3-dimethylaminopropyl)-3-ethylcarbodiimide hydrochloride (EDC) were purchased from Sigma-Aldrich (St. Louis, Missouri, USA). Methyl parathion, parathion, coumaphos, quinalphos, isocarbophos, carbofuran, and deltamethrin were obtained from Beijing Yihuatongbiao Technology Co., Ltd. (Beijing, China). Europium oxide latex microspheres and polyvinylpyrrolidone-K30 (PVP-K30) were purchased from Sinopharm Group Chemical Reagent Co., Ltd. (Beijing, China). The reagents were all analytically pure.

2.2 Instrument

All the aqueous solutions used in the experiment were prepared using an LS-MK2 Pall ultrapure water system (18.2 MΩ cm, New York, USA). The XYZ3050 point-membrane apparatus and the CM4000 strip cutters used to make the TRFIA strips were manufactured by Biodot (California, USA). The TRFIA strips were dried in a DHG-9070A oven manufactured by Shanghai Yiheng Technology Co., Ltd. (Shanghai, China). The CF16RX high-speed refrigerated centrifuge used for the coupling process of Eu-SaMIgGs was manufactured by Hitachi (Tokyo, Japan). The ultrasonic machine for rapid dispersion and mixing of solution was produced by Shanghai Kedao Ultrasonic Instrument Co., Ltd. (Shanghai, China). The microplate reader was produced by Seymour Fisher Technology Co., Ltd. (Iowa, USA). The EOS 6D digital SLR camera used in the experiment was purchased from Canon (China) Co., Ltd. (Beijing, China). The ZF-1 UV-lamp (365 nm) was purchased from Haimen Kylin-Bell Lab Instruments Co., Ltd. (Jiangsu, China). The NC membrane (HF135) and absorbent pad (CFSP223000) were purchased from Millipore Corporation (Massachusetts, USA). The glass cellulose film (GFCP2030) and polyvinyl chloride plate (J-86) were produced by Shanghai Jiening Biotechnology Co., Ltd. (Shanghai, China).

2.3 Preparation of Eu-SaMIgGs

The europium oxide latex microspheres were evenly dispersed by adding 50 μL europium oxide latex microspheres to 200 μL borate buffer solution (0.2 M, pH 8.18), and ultrasonicated at 10 °C for 10 min. The carboxyl groups on the europium oxide latex microspheres were fully activated by adding 10 μL EDC solution (1.5%, m/v) and eddy mixing for 15 min. The mixed solution was centrifuged for 10 min (10 °C, 13 300 rpm), and then the supernatant was discarded. Because the centrifugation product easily redissolves, the centrifuge tube should be removed quickly and smoothly after centrifugation. Then 250 μL of fluorescence microsphere blocking solution (0.05% OVA, m/v) was added and ultrasonicated for 10 min at 10 °C to disperse the solution evenly. A certain dose of SaMIgG was added, and the reaction was carried out on a shaking table for 12 h (20 °C, 250 rpm) after eddy mixing. In this process, the amino group on SaMIgG was fully combined with the carboxyl group on the surface of the europium oxide latex microspheres to form an amide bond, and then Eu-SaMIgGs were prepared (Fig. 1A). At this time, the solution might contain SaMIgG which had not been coupled to the europium oxide latex microspheres. In order to ensure the subsequent smooth preparation of Eu-SaMIgGs-Abs, a re-suspension operation was needed to remove the SaMIgG not coupled with europium oxide latex microspheres in the solution. The mixed solution was centrifuged for 10 min (10 °C, 13 300 rpm), and the supernatant was discarded. The above resuspension operation was repeated twice to ensure full clearance. Then, 250 μL of fluorescence microsphere sealing solution was added, and the mixture was vortex mixed, and ultrasonication treatment was performed at 10 °C for 10 min. Finally, the prepared Eu-SaMIgGs were evenly dispersed in the solution after 2 h shaking reaction (20 °C, 250 rpm), and sealed and stored at 4 °C in the dark.

2.4 Fabrication of the strip

First, a NC membrane (25 mm × 300 mm) was assembled onto a polyvinyl chloride plate (90 mm × 300 mm) in the position shown in Fig. 1B for spraying OPs-BSA and RaSIgG. Methanol and ultra-pure water were used to clean the capillary sample channel on the point-membrane apparatus repeatedly and adequately to prevent the channel from clogging. OPs-BSA and RaSIgG were sprayed on the NC membrane, respectively, to

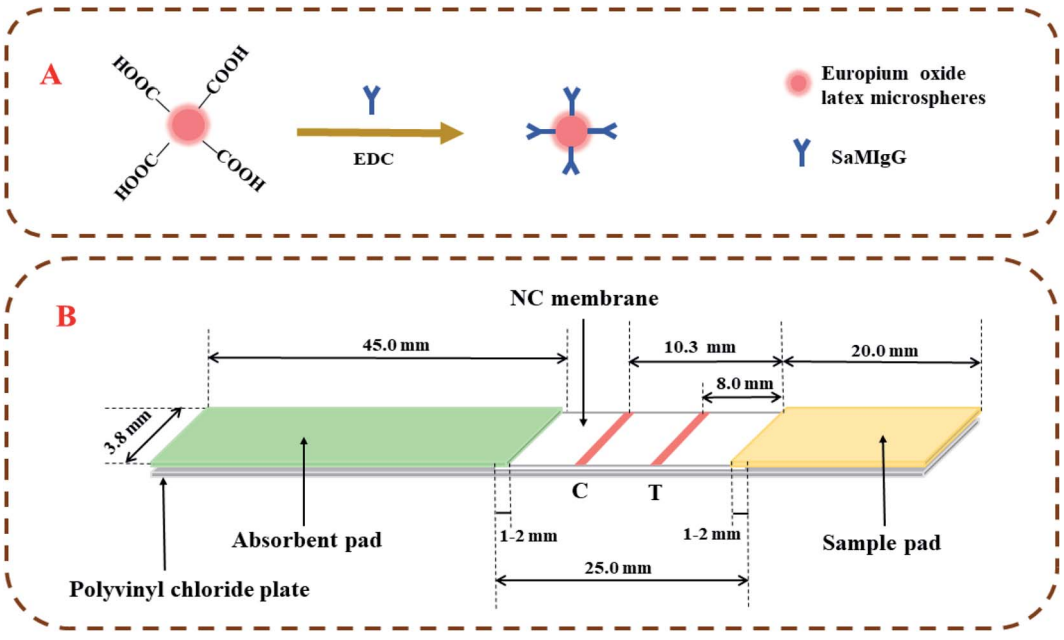

Fig. 1 Diagram of preparation of Eu-SaMIgGs (A) and the structure of the TRFIA strip (B).

form a T-line and a control line (C-line), and dried in an oven at 37 °C for 2 h. At the same time, the glass cellulose film (*i.e.* sample pad, 20 mm × 300 mm) was placed in a clean and dry test tube, and an appropriate amount of sample pad sealing solution (0.3% $NaH_2PO_4 \cdot 2H_2O$, 0.5% OVA, 1.0% PVP-K30, 2.9% $Na_2HPO_4 \cdot 12H_2O$, 1.0% Tween-20, and 0.25% EDTA, m/v) was added to completely cover it. After soaking for 15 min, the film was taken out and placed flat in an oven, and dried at 37 °C for 2 h. After drying completely, as shown in Fig. 1B, the absorbent pad (45 mm × 300 mm) and the sample pad were assembled to the front of the bottom plate. The adjacent parts should be overlapped by 1–2 mm. They are placed at 4 °C for 15–20 min, to be firmly bonded, using a cutting machine at a width of 3.8 mm per strip, then the TRFIA strip product is stored and sealed at 4 °C.

2.5 OP detection on the TRFIA strip

Eu-SaMIgGs-Abs were prepared 30 min before the test. Eu-SaMIgGs-Abs were prepared by fully mixing the sample sustained-release solution (1.0% sucrose, 0.5% OVA, 0.5% PVP-K30, and 2.5% Tween-20, m/v) with Eu-SaMIgGs in a certain volume proportion, adding a certain volume of Abs, and incubating at 37 °C for 30 s. The above steps need to be performed now, and should not be too long apart from the detection steps, in order to avoid the partial quenching of the fluorescence signal of europium oxide latex microspheres which affects the subsequent detection results.

20 μL Eu-SaMIgGs-Abs is added to each sample cell, and then 100 μL sample solution to be tested is added. After incubating at 37 °C for 3 min, Eu-SaMIgGs-Abs specifically bonded with OPs to form the Eu-SaMIgGs-Abs-OPs complex. Eu-SaMIgGs-Abs, which were not combined with OPs, still maintained the original structure. In a dark environment at 37 °C, the TRFIA strip was inserted into the sample cell for 15 min.

In this process, the TRFIA strip should always remain vertical to avoid the difference in tomographic velocity due to tilt. During incubation, the solution in the sample cell was expanded on the NC membrane due to chromatography. OPs-BSA fixed at the T-line could compete with OPs for the same specific binding site on Abs. The RaSIgG immobilized at the C-line specifically recognized the SaMIgGs in Eu-SaMIgGs-Abs. During the chromatographic process, Eu-SaMIgGs-Abs without the binding target would be captured at the T-line and C-line successively. As probes gathered, the bands began to show color (Fig. 2). And probes with the binding target could only be captured at the C-line, and the T-line couldn't show any color. A blank control group was set up for each test.

2.6 Data analysis

After the reaction was complete, the TRFIA strips (including the blank control group) were taken out and placed under a UV-light source (wavelength: 365 nm). A digital SLR camera was used to take photos (exposure time: 4 s) of the TRFIA strips in a black box. ImageJ software was used to select the detection strip area, and the gray value of the detection area in the obtained photos was analyzed.

In order to reduce background interference, the change rate of gray value (G) of each sample to be tested was obtained using formula (1):[28]

$$G = \frac{G_0 - G_n}{G_0} \quad (1)$$

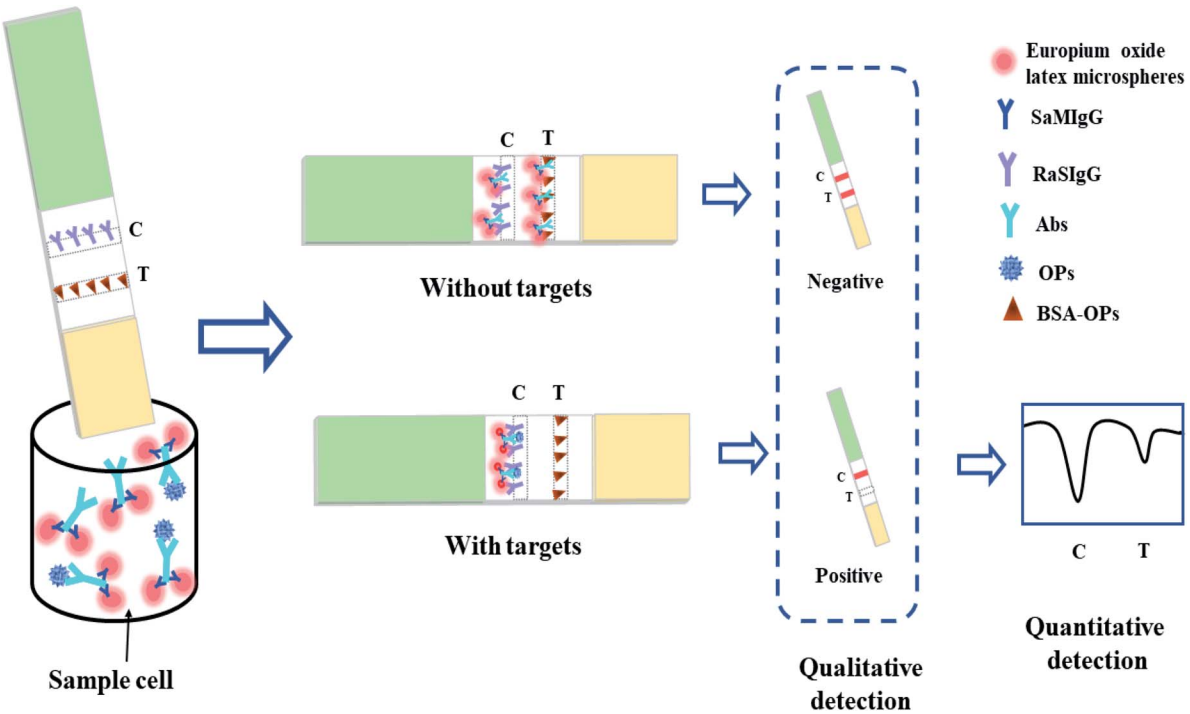

Fig. 2 Schematic diagram of the operation and detection principle of TRFIA strips.

where G is the change rate of the gray value of the sample to be tested, G_n is the gray value of the T-line of the sample solution to be tested, and G_0 is the gray value of the T-line of the blank sample solution.

By exploring the response relationship between the concentration (C) of OPs and the G value of the T-line, the qualitative and quantitative detection of OPs was realized.

2.7 Sample pretreatment

Baby cabbage and rape samples were bought from the local market, and completely pulverized to a homogenate. 25 g of sample homogenate was weighed and 80 mL methanol-PBS (70%, v/v) was added. After the mixed solution was ultrasonicated for 2 min, a uniform filtrate was obtained after filtration through filter paper. The filtrate was centrifuged (10 000 rpm, 5 min), and the supernatant extracted was the sample solution. And it was mixed with PBS buffer solution (0.01 M, pH 7.4) at 1 : 6 (v/v) to obtain the matrix sample solution, which was stored at 4 °C and protected from light for the subsequent test.

3 Results and discussion

3.1 Characterization of Eu-SaMIgGs

UV-vis absorption was performed on both blank europium oxide latex microspheres and Eu-SaMIgGs to demonstrate the successful coupling of europium oxide latex microspheres with SaMIgG (Fig. 3A). No peaks were found in the UV-vis absorption of blank europium oxide latex microspheres, while significant peaks were found in the UV-vis absorption of Eu-SaMIgGs at 220 nm and 260 nm. These results indicate that the europium oxide latex microspheres were successfully coupled with SaMIgG to form Eu-SaMIgGs. In addition, we also scanned the fluorescence spectrum of the europium oxide latex microspheres before and after the coupling with SaMIgG (Fig. 3B). We found that the maximum emission peak was at 614 nm, which indicated that they were europium oxide latex microspheres. However, the wave peak value of europium oxide latex microspheres coupled with SaMIgG decreased slightly compared with that before coupling, as shown in Fig. 3B. The reason was that the europium oxide latex microspheres form a complex after coupling with SaMIgG, which resulted in partial fluorescence signal quenching, that is, fluorescence signal weakening. In the illustration in Fig. 3, the fluorescence signal difference of europium oxide latex microspheres before (Fig. 3B-a) and after (Fig. 3B-b) coupling with SaMIgG is visually shown.

3.2 Optimization of the TRFIA strip

SaMIgG was an important bridge connecting the Abs and europium oxide latex microspheres. When the amount of SaMIgG was too small, all europium oxide latex microspheres cannot be effectively coupled, resulting in waste of labeling materials. However, the addition of too much SaMIgG led to the aggregation of too many protein substances on the surface of europium oxide latex microspheres, resulting in the decrease of fluorescence signal. We tried to add different doses of SaMIgG

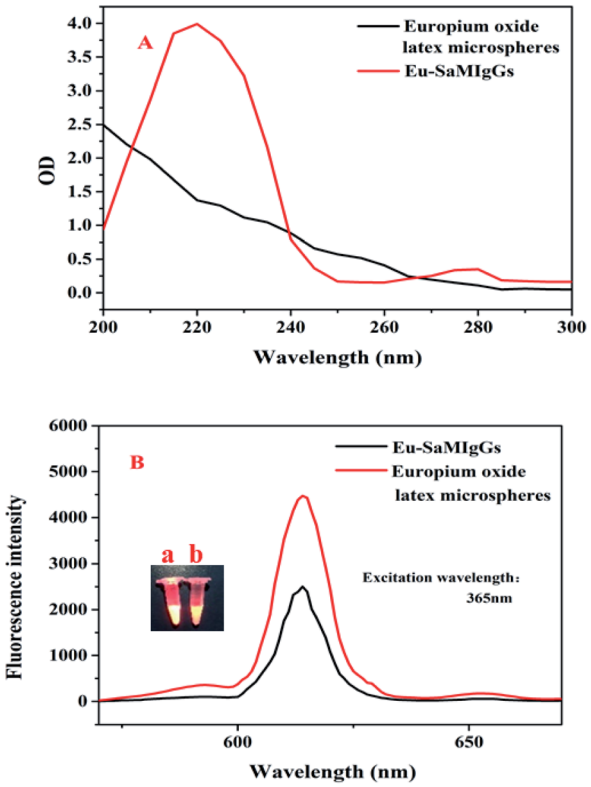

Fig. 3 (A) Uv-vis absorption spectra of europium oxide latex microspheres before and after SaMIgG conjugation. (B) Fluorescence spectra of europium oxide latex microspheres before and after conjugation to SaMIgG; the illustration is a fluorescence picture of the europium oxide latex microspheres before (a) and after (b) the conjugation to SaMIgG.

(10, 15, 20, 25, 30, 35, 40, and 45 μg) when coupling Eu-SaMIgGs, and compared the color development of different C-line positions. As can be seen from Fig. 4A, when the SaMIgG dose was 35 μg, the color development degree of the C-line reached the maximum, and the color development degree remained unchanged even after increasing the dose. Therefore, '35 μg' was chosen as the optimal SaMIgG additive quantity.

Abs were the core recognition element of the TRFIA strip. On the premise of ensuring the detection effect, the main goal of this part was to reduce the consumption of Abs as much as possible. In this work, different doses (1, 2, 4, 6, 8, 10, and 12 μg) of Abs were added to observe the color development of different T-line positions. As shown in Fig. 4B, when the Ab dosage was 6 μg, the color development of the T-line reached the maximum and remained stable. Therefore, '6 μg' was chosen as the best additive value for Abs.

We set up different groups according to the dilution multiples (sample sustained release solution : Eu-SaMIgGs-Abs, v/v) of 10, 20, 40, 80, 30, 640, 1280 and 2560. Fig. 4C shows the effect of the dilution multiples of Eu-SaMIgGs-Abs on the performance of the TRFIA strip. The results show that when Eu-SaMIgGs-Abs was diluted 10 and 20 times, the color of the C-line and T-line was too bright, and a large amount of Eu-SaMIgGs-Abs was stuck on the absorbent pad and NC membrane.

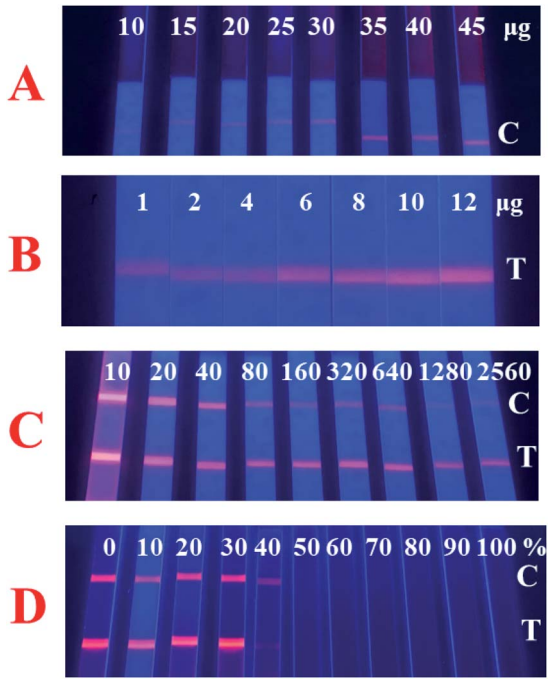

Fig. 4 Optimization of the experimental conditions: (A) the dose of SaMIgG; (B) the amount of Abs added; (C) dilutability; (D) methanol content.

Particularly in the case of '10 times' dilution, the background color of strips had serious interference, which was not beneficial to the extraction of strip data. In the range of 40–640 times dilution, the color of the C-line gradually decreased, indicating that with the increase of dilution, the number of probes that could be combined gradually decreased. At the same time, the color of the T-line remained unchanged, which meant that the OPs-BSA binding ability of the T-line was in a completely saturated state. At 1280 and 2560 times dilution, the color development degree of the C-line was too low to be used as a quality control indication; the color of the T-line also decreased significantly, and OPs-BSA on the T-line was in an unsaturated binding state, resulting in some idle binding sites. Based on the above analysis, when the dilution factor of Eu-SaMIgGs-Abs was set to 640, the binding sites in each band could be fully used to ensure the detection and quality control effect. And it could also save the dosage of Eu-SaMIgGs-Abs.

Methanol was an effective organic solvent for extracting OPs during sample processing. If the concentration of methanol was too low, the pesticide in the sample couldn't be effectively extracted. However, high concentration of methanol would affect antibody biological activity and reduce its recognition ability. Therefore, by studying the tolerance band of Eu-SaMIgGs-Abs to methanol and the effective extraction of OPs in methanol, the appropriate range of methanol concentration was explored. As shown in Fig. 4D, it was found that when the concentration of methanol was between 0 and 30%, the color of the C-line and T-line was normal, that is, the TRFIA strip could work normally. And from 40%, the color of the T-line decreased, or even no color was seen. This indicated that the activity of Eu-SaMIgGs-Abs was inhibited and could not effectively identify OPs-BSA and RaSIgG. In addition, it was found that when the methanol concentration was in the range of 70–100%, a large number of probes adhered to the inner wall of the sample cell due to the volatilization of methanol before the chromatography began. The above results indicated that when the concentration of methanol in the sample solution was in the range of '0–30%', the effective extraction of the sample and the optimal activity of the antibodies could be considered at the same time, and the activity of the antibodies could be reduced or even lost if the concentration of methanol was beyond this range.

3.3 Detection of OPs

Under the optimal construction and operating conditions, the response relationship between the logarithm of OP concentration (lg C) and the corresponding G value of the T-line was studied. In this work, methyl parathion, parathion, coumaphos, and quintiofos were mixed in equal amounts to get mixed standard solutions, and the initial concentration was 3×10^3 ng g^{-1}, and then diluted 3 times successively to get 7 concentrations. A series of concentrations of mixed standard solutions and negative sample solutions were used to investigate the working standard curve of TRFIA strips. The G value of each TRFIA strip was obtained in accordance with formula (1), and the competitive suppression curve suitable for the strip was obtained after analysis, as shown in Fig. 5A. The equation of the curve was $G = 0.99789–1.04464/[1 + (\lg C/3.41689)]^{0.74527}$, R^2 was 0.99853, and the sensitivity was 3.42 ng g^{-1}. With the increase

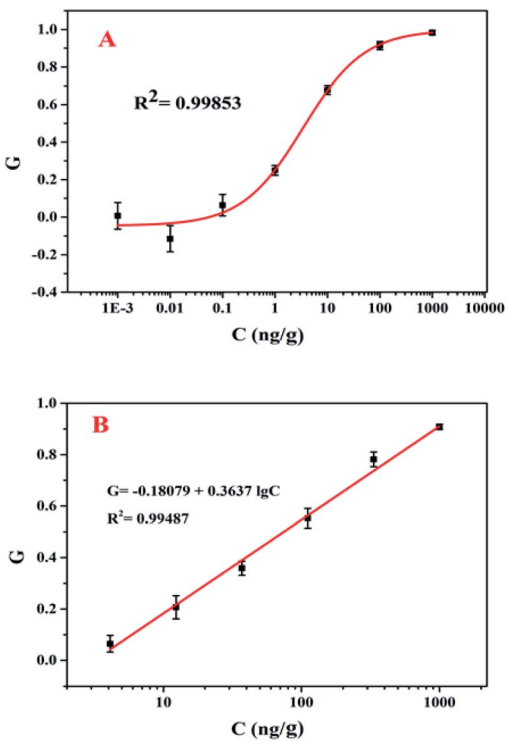

Fig. 5 (A) Competitive inhibition curve and (B) standard curve of the OPs.

Table 1 Comparison with other types of strips

Signal molecule	Strategy	Targets	LOD (ng g^{-1})	Sample types	Ref.
Fe_3O_4	Indirect probe	17β-estradiol	0.2	4	26
Up-conversion luminescent particles	Direct probe	OPs	3.44	3	29
Europium oxide latex microspheres	Indirect probe	Deoxynivalenol	0.12	2	19
Europium oxide latex microspheres	Direct probe	AFM1	0.20	3	24
Europium oxide latex microspheres	Indirect probe	OPs	0.53	4	This work

of target concentration, the number of Eu-SaMIgGs-Abs to OPs-BSA at the T-line that could compete decreased. So, the color rendering degree of the T-line decreased, and led to the increase of the G value. Since 'false positives' or 'false negatives' were easy to occur at both ends of the competitive inhibition curve, we explored the linear relationship between C and G values in the linear range (Fig. 5B), and obtained the linear equation $G = -0.18079 + 0.3637\lg C$, R^2 was 0.99487. According to S/N = 3, the LOD of the TRFIA strip was 0.53 ng g^{-1}.

In Table 1, the TRFIA strip is compared with other types of strips. The results show that the LOD of the TRFIA strip using the indirect probe strategy is significantly lower than that using the direct probe strategy. In addition, the TRFIA strip in this study had a wide target recognition range, low LOD, and a wide variety of sample substrates.

3.4 Performance test of the TRFIA strip

Specificity and anti-interference ability are important indexes to evaluate whether a TRFIA strip could be effectively applied to detection. Under the condition of the same concentration of spiked substances, the TRFIA strip was used to detect the target substances of different OPs or the interfering substances of other pesticides. By analyzing the gray value of the T-lines, the specificity and anti-interference ability of the strip were explored. The blank group (Fig. 6-a) was established as the control. Fig. 6-b shows parathion standard solution. Fig. 6-c is the isocarbophos standard solution, which is an OP but wasn't included in the mixed standard solution. Fig. 6-d is the mixed standard solution (parathion, coumaphos, quintiofos, and methyl parathion). Fig. 6-e shows the mixture of OPs (methyl parathion, parathion, coumaphos, and quintiofos) and non-OPs (carbofuran and deltamethrin). In addition, a carbamate pesticide – carbofuran (Fig. 6-f) – and a pyrethroid pesticide – deltamethrin (Fig. 6-g) – were used as interfering pesticides. The total concentration of OPs in experimental groups b, c, d, and e was 10 ng g^{-1}. And in experimental groups f and g, the concentrations of carbofuran and deltamethrin were both 10 ng g^{-1}. As could be seen from Fig. 6, in the absence of specific targets, the color development of the T-line was close to that of the blank group, indicating that it was difficult for the antibodies to bind to these interfering pesticide molecules. The gray values in Fig. 6-b–e are all low, and the results are close to each other. It indicated that the strip had good specificity and anti-interference ability.

3.5 Detection of OPs in samples

We bought baby cabbage and rape from the market as representatives of vegetable samples. Matrix sample solutions were prepared in accordance with Section 2.7 for sample tests, so as to evaluate the application effect of the TRFIA strip constructed in this study. We adopted the standard addition method to add different volumes of mixed standard solutions to the non-matrix sample solution (*i.e.* 10% methanol-PBS) and two different matrix sample solutions, so that the series concentration gradient of each group of sample solutions was consistent. The TRFIA strip was used to explore the competitive inhibition curve of the sample solution. The experimental results are shown in

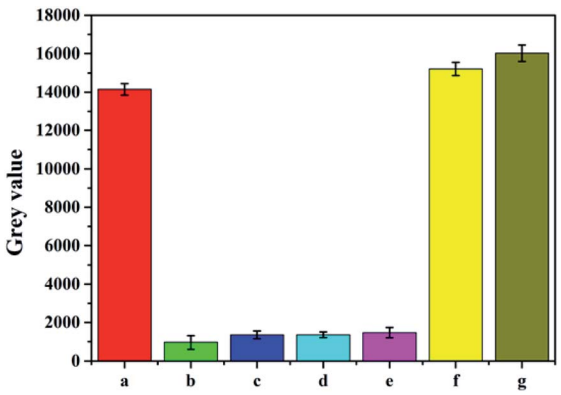

Fig. 6 Performance evaluation of the TRFIA strips (a, blank; b, parathion; c, isocarbophos; d, parathion, coumaphos, quintiofos, methyl parathion; e, parathion, coumaphos, quintiofos, methyl parathion, carbofuran, deltamethrin; f, carbofuran; g, deltamethrin).

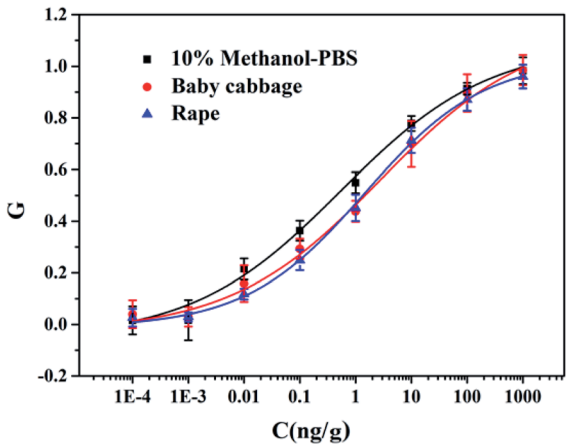

Fig. 7 Competitive inhibition curves for the determination of OPs in samples.

Fig. 7. The sensitivity values of all the matrix solutions were slightly higher than those of the sample solutions without the matrix because the matrix components were complex and varied, which might block the capillary channels in different degrees during the process of chromatography. In the detection experiment for vegetable samples, the competitive inhibition curve of 'baby cabbage' and 'rape' was basically consistent with that of the non-matrix sample solution. However, due to the presence of the green pigment in the substrate solution of rapeseed, there was some background interference during data extraction, resulting in the detection range of rape being slightly narrower than that of 'baby cabbage'. In the process of sample detection using the strip, a material that could adsorb the pigment should be added in the pretreatment to further reduce the interference.

4 Conclusions

Based on the indirect probe strategy, we developed a broad-specificity TRFIA strip for detection of OPs. Europium oxide latex microspheres were used as fluorescent labeling materials to reduce background color interference. Eu-SaMIgGs-Abs was formed by linking europium oxide latex microspheres with Abs using SaMIgG as an intermediate. This strategy could save the amount of target antibodies, effectively realize the amplification of fluorescence signal, and finally improve the sensitivity. More importantly, the secondary antibodies replaced Abs to participate in the complicated coupling steps, which avoided the decline of the biological activity and specific recognition ability of Abs. Under the optimal conditions, the lg C value had a good linear relationship with the G value, and the LOD could reach 0.53 ng g^{-1}. At the same time, the detection effect of the TRFIA strip in different sample matrix solutions was explored to compare and analyze the suitable samples of the sensor. The TRFIA strip established in this work could realize qualitative and quantitative detection. When the strip was applied to a large number of samples, the negative samples could be directly judged with the help of UV-light. And the positive samples could be quickly screened out for quantitative detection, which significantly improved the detection efficiency. The TRFIA strip had the advantages of low cost, short detection time, simple operation, and low professional requirements, and could better meet the needs of rapid preliminary screening of mass samples. Admittedly, due to the limitation of professional background knowledge, the research of this work was only limited to the research of detection technology. Follow-up research could focus on the development of a matching rapid detection instrument and mobile APP, which would be able to present the test results to users more quickly and clearly. This is also conducive to the promotion and application of this work.

Author contributions

Haowei Dong, conceptualization. Ideas; formulation or evolution of overarching research goals and aims. Deyan Xu, investigation. Conducting the research and investigation process, specifically performing the experiments, or data/evidence collection. Guanjie Wang, formal analysis. Application of statistical, mathematical, computational, or other formal techniques to analyze or synthesize study data. Xiaoya Meng, visualization. Preparation, creation and/or presentation of the published work, specifically visualization/data presentation. Qingqing Yang, writing – review & editing. Preparation, creation and/or presentation of the published work by those from the original research group, specifically critical review, commentary or revision – including pre- or post-publication stages. Xia Sun, resources. Provision of study materials, reagents, materials, patients, laboratory samples, animals, instrumentation, computing resources, or other analysis tools. Yemin Guo, funding acquisition. Acquisition of the financial support for the project leading to this publication. Yelong Zhu, supervision. Oversight and leadership responsibility for the research activity planning and execution, including mentorship external to the core team.

Conflicts of interest

There are no conflicts to declare.

Acknowledgements

This work was supported by the National Natural Science Foundation of China (31772068), Special Project of Independent Innovation of Shandong Province (2018CXGC0214), and Zibo-Sdut Integration Development Project (2019ZBXC090).

Notes and references

1 J. Fu, X. An, Y. Yao, Y. Guo and X. Sun, *Sens. Actuators, B*, 2019, **287**, 503–509.
2 H. Liu, X. Bai and X. Pang, *Sci. Total Environ.*, 2020, **700**, 134481.
3 R. Bala, S. Dhingra, M. Kumar, K. Bansal, S. Mittal, R. K. Sharma and N. Wangoo, *Chem. Eng. J.*, 2017, **311**, 111–116.
4 R. H. Wang, C. L. Zhu, L. L. Wang, L. Z. Xu, W. L. Wang, C. Yang and Y. Zhang, *Talanta*, 2019, **205**, 120094.
5 Z.-l. Chen, F.-s. Dong, J. Xu, X.-g. Liu and Y.-q. Zheng, *J. Integr. Agric.*, 2015, **14**, 2319–2327.
6 P. Parrilla Vázquez, C. Ferrer, M. J. Martínez Bueno and A. R. Fernández-Alba, *TrAC, Trends Anal. Chem.*, 2019, **115**, 13–22.
7 G. Pang, Q. Chang, R. Bai, C. Fan, Z. Zhang, H. Yan and X. Wu, *Engineering*, 2020, **6**, 432–441.
8 P. Sivaperumal, P. Anand and L. Riddhi, *Food Chem.*, 2015, **168**, 356–365.
9 M. Liu, A. Khan, Z. Wang, Y. Liu, G. Yang, Y. Deng and N. He, *Biosens. Bioelectron.*, 2019, **130**, 174–184.
10 C. S. Pundir, A. Malik and Preety, *Biosens. Bioelectron.*, 2019, **140**, 111348.
11 A. Khanmohammadi, A. Aghaie, E. Vahedi, A. Qazvini, M. Ghanei, A. Afkhami, A. Hajian and H. Bagheri, *Talanta*, 2020, **206**, 120251.
12 F. Arduini, S. Cinti, V. Caratelli, L. Amendola, G. Palleschi and D. Moscone, *Biosens. Bioelectron.*, 2019, **126**, 346–354.

13 M. Liu, A. Khan, Z. F. Wang, Y. Liu, G. J. Yang, Y. Deng and N. Y. He, *Biosens. Bioelectron.*, 2019, **130**, 174–184.
14 H. Dong, Q. Zhao, J. Li, Y. Xiang, H. Liu, Y. Guo, Q. Yang and X. Sun, *Bioprocess Biosyst. Eng.*, 2021, **44**, 585–594.
15 Z. L. Xu, H. Wang, Y. D. Shen, M. Nichkova, H. T. Lei, R. C. Beier, W. X. Zheng, J. Y. Yang, Z. G. She and Y. M. Sun, *Analyst*, 2011, **136**, 2512–2520.
16 Z.-L. Xu, Y.-D. Shen, W.-X. Zheng, R. C. Beier, G.-M. Xie, J.-X. Dong, Y. Jin-Yi, H. Wang, H.-T. Lei, Z.-G. She and Y.-M. Sun, *Anal. Chem.*, 2010, **82**, 9314–9321.
17 Z. L. Xu, G. M. Xie, Y. X. Li, B. F. Wang, R. C. Beier, H. T. Lei, H. Wang, Y. D. Shen and Y. M. Sun, *Anal. Chim. Acta*, 2009, **647**, 90–96.
18 Z. Zhang, D. Wang, J. Li, Q. Zhang and P. Li, *Anal. Methods*, 2015, **7**, 2822–2829.
19 H. Dong, X. An, Y. Xiang, F. Guan, Q. Zhang, Q. Yang, X. Sun and Y. Guo, *Sensors*, 2020, **20**, 6577.
20 J. Yu, T. Guo, W. Zhang, Y. Zhu, B. Li and R. Hua, *Mater. Res. Bull.*, 2019, **111**, 133–139.
21 A. E. Urusov, A. V. Petrakova, A. V. Zherdev and E. A. Zvereva, *Open Biotechnol. J.*, 2019, **13**, 113–121.
22 K. Li, X. Li, Y. Fan, C. Yang and X. Lv, *Sens. Actuators, B*, 2019, **286**, 272–281.
23 F. Zhu, H. Zhang, M. Qiu, N. Wu, K. Zeng and D. Du, *Sci. Total Environ.*, 2019, **695**, 133793.
24 M. Li, H. Wang, J. Sun, J. Ji, Y. Ye, X. Lu, Y. Zhang and X. Sun, *Food Control*, 2021, **121**, 107616.
25 G. Li, D. Wang, A. Zhou, Y. Sun, Q. Zhang, A. Poapolathep, L. Zhang, Z. Fan, Z. Zhang and P. Li, *J. Agric. Food Chem.*, 2018, **66**, 5671–5676.
26 X. Yao, Z. Wang, L. Dou, B. Zhao, Y. He, J. Wang, J. Sun, T. Li and D. Zhang, *Sens. Actuators, B*, 2019, **289**, 48–55.
27 M. Majdinasab, M. Zareian, Q. Zhang and P. Li, *Food Chem.*, 2019, **275**, 721–729.
28 M. Tian, W. Xie, T. Zhang, Y. Liu, Z. Lu, C. M. Li and Y. Liu, *Sens. Actuators, B*, 2020, **309**, 127728.
29 R. Zou, Y. Chang, T. Zhang, F. Si, Y. Liu, Y. Zhao, Y. Liu, M. Zhang, X. Yu, X. Qiao, G. Zhu and Y. Guo, *Front. Chem.*, 2019, **7**, 18.